40Ar/39Ar geochronology of magmatism and hydrothermal activity of the Madjarovo base-precious metal ore district, eastern Rhodopes, Bulgaria

Peter Marchev and Brad Singer

Geological Society, London, Special Publications 2002; v. 204; p. 137-150
doi:10.1144/GSL.SP.2002.204.01.09

$^{40}Ar/^{39}Ar$ geochronology of magmatism and hydrothermal activity of the Madjarovo base–precious metal ore district, eastern Rhodopes, Bulgaria

PETER MARCHEV[1] & BRAD SINGER[2]

[1]*Geological Institute, Bulgarian Academy of Sciences, Acad. G. Bonchev St., Bl.24, 1113 Sofia, Bulgaria (e-mail: pmarchev@router.geology.bas.bg)*

[2]*Department of Geology and Geophysics, University of Wisconsin-Madison, 1215 West Dayton St., Madison, WI 53706, USA*

Abstract: The Madjarovo volcanic complex and ore district comprise alteration styles from potassium silicate, advanced argillic and sericite alteration to adularia–sericite alteration/mineralization with a close and unambiguous spatial relationship to specific magmatic events. New $^{40}Ar/^{39}Ar$ laser fusion and incremental heating experiments on nine sanidine, biotite, adularia, K-feldspar, and alunite samples constrain the ages and time span of lavas and tephras comprising the complex and their relationship to the hydrothermal activity. These results demonstrate that high-K calc-alkaline to shoshonitic volcanic activity began *c.*32.7 Ma and terminated *c.*500 ka later with the extrusion of quartz latite lavas at 32.2 Ma. The final stage of volcanism was accompanied by intrusion of compositionally similar monzonite stocks and trachytic dykes (*c.*32.2–32.1 Ma) and associated barren advanced argillic and sericite alteration (lithocap) and adularia–sericite base/precious metal vein mineralization. A probable thermal event at *c.*12–13 Ma disturbed the ages of alunite and sericite-bearing alteration at low stratigraphic levels. However, field relations combined with a plateau age of 32.1 ± 0.2 Ma from adularia in low-sulphidation veins that cross-cut lithocap indicate that hydrothermal activity, including base- and precious-metal vein deposition, was coeval with the youngest magmatic activity.

Although most recent models of epithermal systems emphasize close spatial association among volcanic and plutonic events, alteration, and deposition of ore (Hedenquist & Lowenstern 1994; Sillitoe 1993, 1995), only rare combinations of geological events provide examples where relationships between igneous rocks, porphyry and epithermal systems (both high and low sulphidation) are exposed. This is mainly because young epithermal systems are poorly exposed, whereas older deposits are eroded or deformed (Hedenquist & Arribas 1999; Cooke & Simmons 2000). Most economic epithermal ore deposits are Tertiary and conventional K–Ar dating cannot precisely constrain the timing of magmatism, alteration, and mineralization. At the 95% confidence level the precision of $^{40}Ar/^{39}Ar$ age determinations of K-rich minerals is typically better than ± 0.5%, thus for the Oligocene materials of this investigation differences in age of about 200 ka may be distinguished (e.g. Marsh *et al.* 1997; Singer & Marchev 2000).

Mining at Madjarovo ore district in Bulgaria is believed to have commenced during Thracian times, with most development beginning in the 1950s. More than 10 million tons of base metal ore have been mined; another 6.5 million tons of base metal reserves and low-grade ore still exist. However, because of changes in the Bulgarian economy and a decrease in ore grade with depth, mining for base metals has ceased. Jambol Exploration Organization undertook an extensive gold exploration programme of the upper parts of the base metal veins between 1988 and 1996. Eight major veins contain reserves of *c.* 2 million tons grading 3.9 g t^{-1} Au, but a 1995 feasibility study by Euraust Mineral Developments indicated that the deposit is not economic for Au.

We chose to focus on the Madjarovo ore district because the Arda River has dissected the whole volcanic complex and ore district, exposing the close spatial relationships between porphyry monzonite stocks and dykes in the central part of the complex and potassic, barren acid–sulphate (advanced argillic) and adularia–sericite (low-sulphidation) alteration and accompanied base/precious metal mineralization. This geological setting provides an excellent opportunity to constrain the timing and

From: BLUNDELL, D.J., NEUBAUER, F. & VON QUADT, A. (eds) 2002. *The Timing and Location of Major Ore Deposits in an Evolving Orogen*. Geological Society, London, Special Publications, **204**, 137–150.
0305-8719/02/$15.00

duration of magmatic and hydrothermal events using $^{40}Ar/^{39}Ar$ methods. Our new age determinations support a close connection between magmatic events and hydrothermal alteration and potential contemporaneity of the contrasting fluids responsible for barren advanced argillic/sericitic alteration and adularia–sericite alteration/mineralization.

Geological setting

Regional setting

The Madjarovo ore district of southeastern Bulgaria is situated approximately 200 km SE of Sofia (Fig. 1) in the centre of the Oligocene Madjarovo volcano. The volcano itself is the easternmost volcanic structure on the Bulgarian territory of an Eocene–Oligocene continental magmatic belt that extends *c.* 500 km from Serbia and Macedonia to NW Turkey (Fig. 1). The magmatic belt resulted from post-Palaeocene–Eocene extension that followed Upper Cretaceous collision of the Serbo-Macedonian and Rhodope Massifs with the Pelagonian microplate (Ricou 1994). The eastern part of this belt is occupied by the Rhodope Massif, which is comprised of Precambrian to Mesozoic metamorphic rocks. Palaeogene magmatic rocks consist of calc-alkaline to shoshonitic intermediate, acid and subordinate basic volcanic rocks and their intrusive equivalents (Ivanov 1968; Innocenti *et al.* 1984; Harkovska *et al.* 1989; Del Moro *et al.* 1990; Christofides *et al.* 1998; Marchev *et al.* 1998*a*; Yanev *et al.* 1998), showing a distinct south to north enrichment (from Greece to Bulgaria) in K_2O and LILE. Minor alkali basalts have been described in the southeastern part of the Eastern Rhodopes (Marchev *et al.* 1998*b*). The Palaeogene magmatism was accompanied by the formation of small Cu–Mo and abundant epithermal deposits (Mavroudchiev *et al.* 1996; Arikas & Voudouris 1998), which form the Rhodope metallogenic province (Stoyanov 1979).

District geology

The Madjarovo volcanic complex covers 120 km^2. New geological mapping at 1:10 000 is summarized in Figure 2. Pre-Tertiary rocks, that crop out south of the Chernichevo Fault, are overlain by Upper Priabonian conglomerate, sandstone and limestone. A tephrostratigraphic marker, composed of pumice and ash-fall tuff of unknown source, named the Reseda Tuff (Ivanov & Kopp 1969), overlies these sediments and underlies the Madjarovo volcanic complex. The Arda river, exploiting a large east–west fault (Arda zone), exposes the deep stratigraphy of the volcano. Volcanism was predominantly fissure-fed and dominated by large sheet-like lava flows and subordinate epiclastic rocks that formed a shield volcano (Ivanov 1960). The unaltered mafic to intermediate volcanic rocks (Marchev *et al.*1989) are shoshonitic to high-K calc-alkaline rocks dominated by latites. Burchina quartz latites are

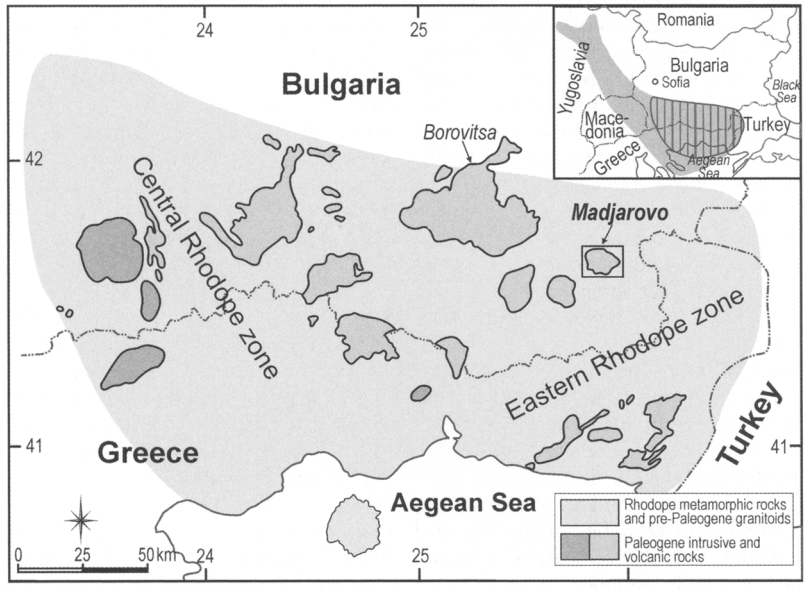

Fig. 1. Location of Eocene Madjarovo volcanic complex within the Palaeogene intrusive and volcanic belt, Rhodope Mountians. Inset shows the Palaeogene Macedonian–Rhodope–North-Aegean Volcanic Belt.

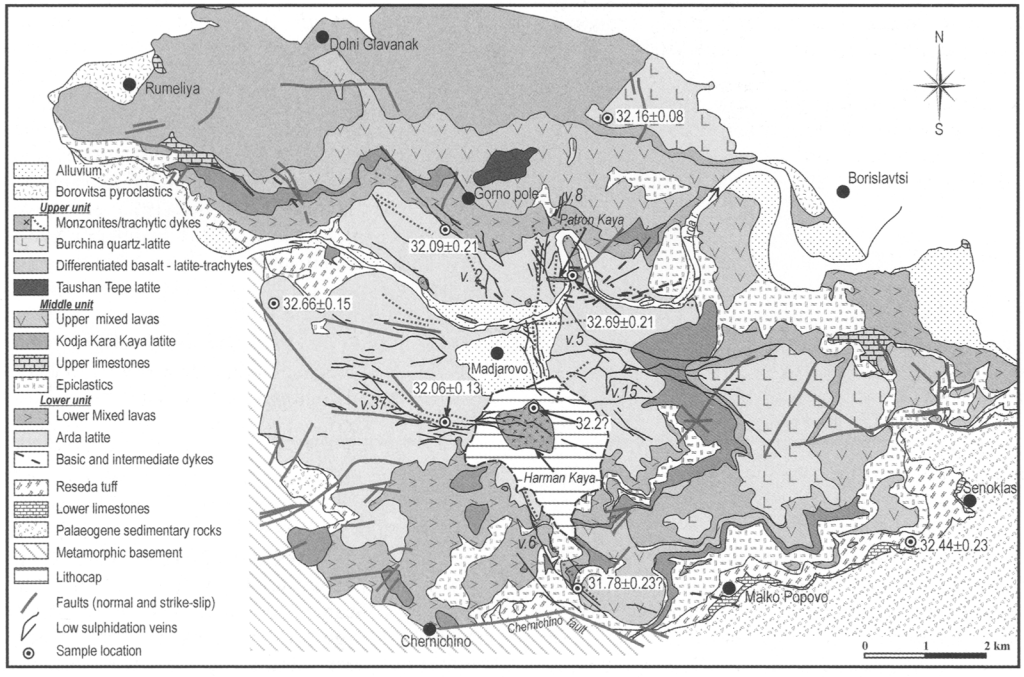

Fig. 2. Simplified geological map of the Madjarovo ore district, showing sample locations and their preferred ages. Source: unpublished mapping by P. Marchev, 1989–1995.

the youngest volcanic rocks. They are overlain by another tephrostratigraphic marker, Borovitsa rhyolite tuff, which is an outflow tuff originated from Borovitsa caldera located 20 km WNW of Madjarovo (Singer & Marchev 2000).

On the basis of petrology and Sr and O isotope compositions (Marchev & Rogers 1998), three units have been divided within the Madjarovo complex. The first two (Lower and Middle unit) start with thick (up to 150 m) latites and end with basalts. Less voluminous intercalated flows of basaltic andesites, shoshonites and andesites show petrographic and isotopic evidence for large-scale magma mixing between end-members (Raicheva *et al.* 2001). The third unit includes three lavas ranging from high-K high-Al basalt through latite and quartz-latite.

Early volcanic rocks are intruded by numerous monzonitic stocks and rare gabbroic and syenitic bodies, similar in composition to the Upper unit. It is presumed that the monzonite stocks coalesce at depth (Mavroudchiev 1959). The largest monzonitic body, Harman Kaya, and trachytic dykes of identical composition crop out in the central part of the complex over 40–50 km^2. A gravity minimum and magnetic anomaly beneath the centre of the complex have been interpreted as a syenitic pluton between depths of 1 and 4 km (Iosifov *et al.*1987). Intrusion of monzonite-trachyte magma was accompanied and followed by destruction of the central part of the volcano. Gergelchev (1974) postulated the existence of a caldera structure coinciding in size with the pluton, but the results of extensive drilling and our field observations did not confirm this interpretation.

Four major fault systems, striking east–west, NW–SE, north–south and NE–SW (Atanasov 1959; Velinov *et al.* 1977), accommodate the feeding dyke swarms for the lavas, sub-volcanic intrusions and the base/precious metal veins and alteration, suggesting that these structures controlled volcanism and subsequent mineralization. The most prominent structures are the east–west Chernichevo fault delimiting the metamorphic and volcanic rocks in the southern part of the volcano (Fig. 2), and the east–west Arda structural zone. A series of faults between them bound blocks tilted to the NNE and decreasing in altitude northward with total displacements of up to 600–700 m. The richest veins (e.g., #2, 6, 8; Fig. 2) also represent faults with displacement up to 200 m (Atanasov 1959). They show abundant evidence of brecciation and recementation, suggesting movement during ore deposition. However, preservation of the epithermal zonation in the

elevated southern and down-dropped northern halves of the complex suggests that the current structure most probably developed synchronously with trachyte/monzonite intrusions and that ore deposition post-dated most deformation.

Alteration

Alteration in the Madjarovo ore district is documented by Radonova (1960), Velinov *et al.* (1977), Velinov & Aslanian (1981), Velinov & Nokov (1991) and Marchev *et al.* (1997). Current knowledge of hydrothermal alteration is summarized in McCoyd (1995) and herein. The epithermal system generated acid–sulphate and adularia–sericite alteration (Velinov & Nokov 1991) and subjacent K-silicate alteration (Marchev *et al.* 1997). Skarns were discovered by drilling near the Harman Kaya and Patron Kaya monzonite stocks (Breskovska *et al.* 1976, Figure 2). McCoyd (1995) subdivided the epithermal alteration into advanced argillic, sericitic, propylitic, quartz–sericite and adularia–sericite; these alteration zones are described below.

K silicate alteration occurs adjacent to two small monzonite stocks in the Arda zone, Patron Kaya and Kjumiurluka (the latter not shown in Fig. 2). It comprises hydrothermal biotite, K-feldspar, albite and quartz. The altered rocks contain disseminated pyrite with rare Cu-bearing (chalcopyrite) mineralization.

Propylitic alteration is developed around K-silicate and sericite alteration over *c.* 10 km^2 in the central part of the district. This alteration was originally designated as pre-ore regional propylitization (Radonova 1960). Propylitic alteration also developed surrounding fracture-controlled base/precious metal vein mineralization. The propylitic assemblage consists of all or some of the following minerals: chlorite, epidote, albite, carbonate and pyrite.

Sericite alteration consisting predominantly of muscovite+quartz accompanied by minor pyrite and dickite, this alteration affected the uppermost Harman Kaya monzonite and its wall rocks (Fig. 2). Sericite alteration forms envelopes around zones of advanced argillic alteration, together forming a lithocap (Sillitoe 1995), which probably at depth passes into K-silicate alteration. A large number of base-metal veins occur within the sericitic alteration zone and Harman Kaya monzonite intrusion but the ore grade in the veins diminishes and visible mineralization is not present. This area was determined by Breskovska *et al.* (1976) to be unsuitable for vein type mineralization.

Advanced argillic alteration comprising kaolinite, pyrophyllite, alunite, diaspore and zunyite (Velinov & Nokov 1991; McCoyd 1995), this alteration is in two east–west trending zones in the southern half of the district with alunite alteration occurring at the highest elevation (Fig. 2). The phase assemblage indicates a temperature of *c.* 270 °C, and S isotope geothermometry using an alunite–pyrite pair suggests temperatures of 300–310 °C. Alunite veins located within this alteration are up to 30 cm thick, several metres long, comprise coarse-grained crystals to 150 μm, and strike N130°E. SEM analysis (McCoyd 1995) showed that it consists of woodhousite + svanbergite + alunite. The upper part of the intrusion was silicified locally.

Quartz–sericite alteration is associated with the deeper portions of the base-metal veins, but is also found at higher levels. It is strongly fracture-controlled and forms envelopes around quartz veins. Typically, the width of the zone is a few tens of centimetres but can be up to several metres around larger veins. Quartz and sericite predominate but illite and smectite and disseminated pyrite also occur. Sericite replaces feldspar and also occurs in the groundmass, whereas quartz occurs as veinlets near the main vein deposits.

Adularia–sericite alteration is typical in the upper levels of the palaeo-volcano, it extends up to 120 m on either side of the veins (Fig. 2). It developed either as a halo around large open veins or comprises the brecciated zones. The most intensely altered rocks consist exclusively of a fine-grained aggregate of quartz and adularia. Chemical analyses indicate up to 13 wt% K_2O, suggesting that about 80–85% of the rock is adularia.

Mineralization

The base metal–Au mineralization at Madjarovo is located in the four major fault systems (Fig. 2). Of nearly 150 quartz–sulphide veins that have been identified, 50 veins are economically significant. Vein widths vary from half a metre to thirty metres and the largest of these are up to 3 km long (Fig. 2). Brecciation is typical of the narrowest veins whereas the larger veins are massive and internally banded.

Zoning similar to current models of epithermal deposits, with base metals precipitating below precious metals (Buchanan 1981; Berger & Eimon 1983) was suggested by Atanasov (1962). The mineralized interval persists to 1500 m below the present surface with the precious metal mineralization located in the uppermost 150–200 m. Nu-

merous (>90) primary minerals form the deposit. The predominant sulphides are pyrite, chalcopyrite, Fe-poor sphalerite and Ag-bearing galena with minor Se, Bi, Ag, Sb, As sulfosalts and native Au and Ag (Breskovska & Tarkian 1993). Quartz is the dominant gangue mineral with lesser amounts of barite, chalcedony, jasper and calcite. The paragenesis is complex and six stages of mineralization have been identified (Atanasov 1962; Breskovska & Tarkian 1993). Nokov & Malinov (1993) report findings of molybdenite and hypogene wulfenite in some veins.

Fluid inclusion studies (Breskovska & Tarkian 1993; Nokov & Malinov 1993; McCoyd 1995) have shown that quartz associated with main stage Pb–Zn mineralization was deposited at 240–270 °C from neutral low salinity fluids (3–5 eq. wt% NaCl). Barite associated with the precious-metal mineralization was deposited from similar fluids. Although there is no direct evidence, given the estimated geothermal gradient and occurrence of hydrothermal breccias and adularia, boiling was possible (McCoyd 1995).

Geochronology

Conventional K–Ar dating at Madjarovo broadly constrained the ages of various igneous rocks between 33.5 Ma and 31.0 Ma (Lilov *et al.* 1987). Similarly, Rb–Sr mineral isochrons from the lowermost and uppermost latitic lava flows comprising Madjarovo volcano were 31.6 ± 1.2 Ma and 32.3 ± 0.6 Ma, respectively (Marchev & Rogers 1998). Arnaudova *et al.* (1991) reported a K–Ar age of 33–32 Ma for an adularia sample from the adularia–sericite alteration. A similar age (32.6 ± 1.2 Ma) was obtained by McCoyd (1995) for the vein alunite from the advanced argillic alteration. However, two sericite separates of sericite alteration and one from the quartz–sericite alteration at the southeastern end of vein #2, obtained by the same author, yielded much younger ages (13.0 ± 0.5 Ma–13.7 ± 0.6 Ma) and (12.2 ± 1.0 Ma, respectively. These data, along with the newly obtained $^{40}Ar/^{39}Ar$ data, will be discussed in a later section.

$^{40}Ar/^{39}Ar$ analytical techniques

To define more precisely the timing of igneous and hydrothermal events we undertook $^{40}Ar/^{39}Ar$ experiments on sanidine, biotite, adularia, K-feldspar and alunite from nine samples of volcanic, intrusive and hydrothermal rocks using a CO_2 laser probe. Minerals were separated from 100–250 micron sieve fractions using standard magnetic, density, and handpicking methods. Five milligrams of each mineral were irradiated at Oregon State University for 12 or 50 hours along with 27.92 Ma sanidine from the Taylor Creek rhyolite (Duffield & Dalrymple 1990) as the neutron fluence monitor. Isotopic measurements were made of the gas extracted by either totally fusing individual crystals of < 0.1 mg, or by incrementally heating larger 2–3 mg multi-crystal aliquots using a defocused CO_2 laser beam. The isotopic composition of gas from each fusion or heating step was measured using an MAP 216 spectrometer at the University of Geneva. Six to eleven total fusion measurements were pooled together to calculate a weighted mean age and uncertainty. Incremental-heating results are generally given as weighted mean plateau ages. Analytical procedures, including mass spectrometry, procedural blanks, reactor corrections, and estimation of uncertainties are described by Singer & Marchev (2000). All uncertainties are $\pm 2\sigma$

Samples and results

The results of laser total fusion and incremental heating experiments are summarized in Table 1 and age spectra of the latter are illustrated in Figure 3. The locations of the samples and their preferred ages are shown on the geological map (Fig. 2). The significance and preferred age determined for each sample are as follows.

Reseda Tuff Sample M96-5 is from the Reseda Tuff. Although heavily zeolitized, phenocrysts of sanidine, plagioclase, biotite, sphene and zircon are unaltered and suggest that the source magma was a low-silica rhyolite. Total fusion analyses of six sanidine crystals from a pumice fragment in the upper part of the tuff yielded a weighted mean age of 32.44 ± 0.23 Ma.

Lowermost Arda latite lava flow Sample M96-8 is from the periphery of the complex (Fig. 2) where the lava overlies Reseda Tuff. It contains phenocrysts of plagioclase ($An_{77.5-51}$), augite, orthopyroxene, titanomagnetite, biotite, and minor amphibole and apatite. The weighted mean of eight total-fusion measurements of biotite yielded an age of 32.66 ± 0.15 Ma (Table 1). Sample M92-46 is from the central part of the volcano (Fig. 2) about 50 m from the Patron Kaya monzonite stock. Potassium alteration associated with the stock comprises fine-grained biotite, K-feldspar, albite and quartz pervasively replacing groundmass, plus calcite and chlorite replacement of pyroxene, leaving relict phenocrysts of plagioclase and biotite. Disseminated pyrite and rare chalcopyrite accompany these silicate minerals. Seven of eight total-fusion measurements of unaltered biotite phenocrysts yielded a weighted

Table 1. *Summary of $^{40}Ar/^{39}Ar$ geochronological data for laser fusion and incremental heating experiments on adularia, biotite and sanidine from Madjarovo, Bulgaria*

Sample	Mineral	Description	Total fusion		Incremental heating
			Number of fusions	Weighted mean age (Ma)	'Plateau age'
M96-11	Adularia	Low-sulphidation alteration, vein 6	7 of 9	31.78 ± 0.23	32.57 ± 0.14?
M96-11Pl	Adularia	Low-sulphidation alteration, vein 6			31.12 ± 0.35?
M97-02	Adularia	Low-sulphidation alteration, vein 2	7 of 7	31.91 ± 0.40	32.09 ± 0.21
M96-4	Sanidine	Stratigraphically highest quartzlatite	11 of 11	32.16 ± 0.08	32.23 ± 0.19
4-69	Sanidine	Trachyte dyke	7 of 9	32.06 ± 0.13	
M92-46	Biotite	Stratigraphically lowest latite	7 of 8	32.69 ± 0.21	32.72 ± 0.23
M96-8	Biotite	Stratigraphically lowest latite	8 of 8	32.66 ± 0.15	
M96-5	Sandine	Reseda Tuff	6 of 6	32.44 ± 0.23	

Ages are calculated relative to 27.92 Ma Taylor Creek sanidine (Duffield & Dalrymple 1990). ± 2σ errors.

mean age of 32.69 ± 0.21 Ma (Table 1), whereas a ten-step incremental heating experiment gave a concordant spectrum and a plateau age of 32.72 ± 0.23 Ma that is indistinguishable from the total fusion age (Fig. 4). Neither age is indistinguishable from that of biotite M96-8, moreover the age of Arda latite and Reseda Tuff overlap, suggesting a rapid growth of Madjarovo volcano concomitant with eruption of the tuff.

Uppermost Burchina quartz latite lava flow Sample Md96-4 is from the uppermost Burchina quartz latite that contains phenocrysts of plagioclase ($An_{58.5-41.2}$), sanidine ($Or_{75.1-72.4}$), clinopyroxene; orthopyroxene rimmed by clinopyroxene, biotite, and titanomagnetite, plus zircon and apatite. Eleven total-fusion measurements of sanidine gave a weighted mean age of 32.16 ± 0.08 Ma (Table 1). The plateau age of 32.23 ± 0.19 Ma from a concordant five-step incremental heating experiment is indistinguishable from the total fusion age. Although these ages are in excellent agreement with the 32.3 ± 0.6 Ma clinopyroxene–plagioclase–biotite–sanidine Rb–Sr isochron of Marchev & Rogers (1998), our preferred total fusion age is nearly an order of magnitude more precise.

Trachytic dyke Sample 4-69 is from a trachytic dyke similar in composition and probably coeval with the Harman Kaya monzonite and spatially associated with younger mineralized veins discussed below. Sanidine phenocrysts up to 2.5 cm are common and seven of nine total-fusion measurements yielded a weighted mean age of 32.06 ± 0.13 Ma, that is younger than the Arda latite, but indistinguishable from the Burchina quartz latite age.

Harman Kaya monzonite stock Although sample M89-150 is from the least altered part of the largest monzonite stock (Fig. 2), it is propilitized and dated K-feldspar crystals (up to 2.5 cm) are partly replaced by minor sericite and clay. The 13 step age spectrum is discordant with apparent ages increasing gradually from about 29.85 ± 0.60 Ma in low-temperature steps to the highest temperature step at 31.71 ± 0.26 Ma (Fig. 3). The oldest apparent age approaches that of the younger lava flows and the trachyte dyke. Eight total fusion ages (not shown) range from 30.51 ± 0.64 Ma to 32.24 ± 0.56 Ma with the older of these ages also similar to those of the younger lavas. Given the alteration and discordant age spectrum suggestive of minor loss of radiogenic argon, we take the older age of 32.24 ± 0.56 Ma with caution as our best estimate of time elapsed since rapid cooling of this shallow intrusion.

Adularia–sericite epithermal alteration/mineralization Samples M97-02 and M96-11 are from prominent alteration zones associated with low-sulphidation base-metal–Au veins. M97-02 is from altered latite 2 m from the northern margin of the 25 m wide vein #2 (Fig. 2). Adularia that we measured is a replacement of plagioclase and

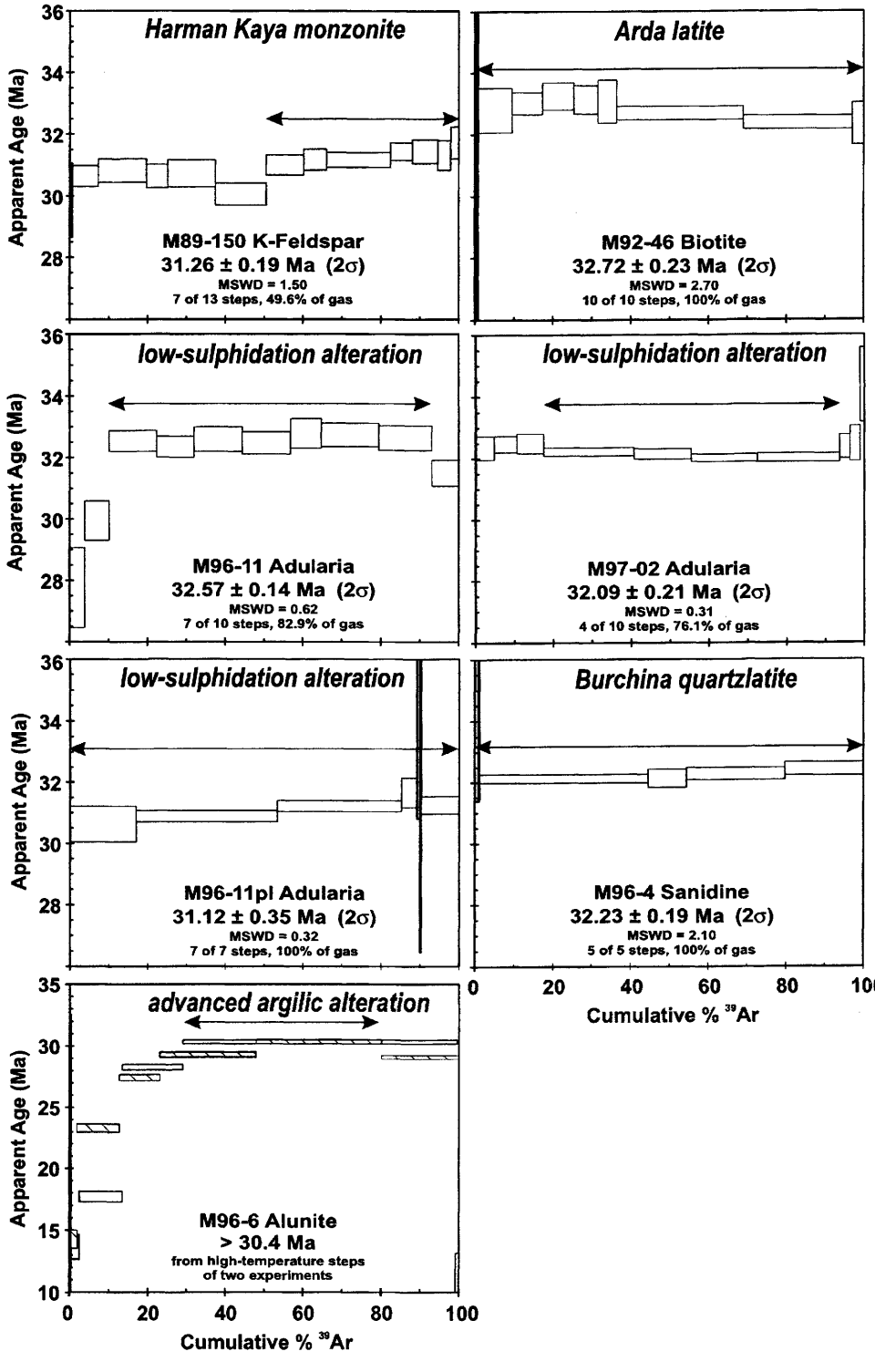

Fig. 3. Age spectra from incremental-heating experiments on sanidine, biotite, K-feldspar, adularia and alunite samples from Madjarovo.

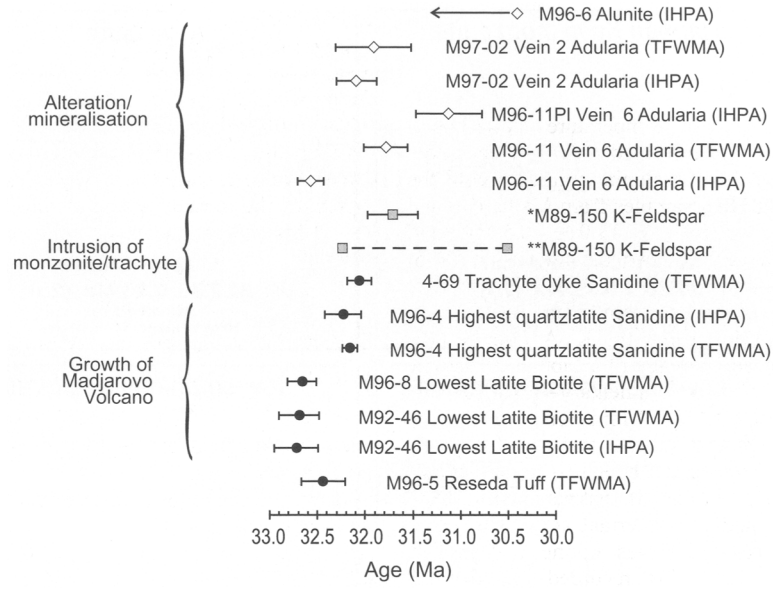

Fig. 4. Summary of preferred ages based on $^{40}Ar/^{39}Ar$ incremental heating and laser fusion results of this study. * K-fs age interval of monzonite based on the total fusion experiments. ** K-Fs age of the highest temperature age of incremental heating experiment. The alunite age is a minimum based on the highest age steps in the age spectra of Figure 3. Abbreviations: TFWMA, total fusion weighted mean age; IHPA, incremental heating 'plateau' age

contains minor sericite. M96-11 is from the breccia in Chatal Kaya vein #6, (Fig. 2) that comprises angular clasts of strongly adularized and silicified shoshonite lava, cemented by veinlets of quartz and ore minerals. The adularia occurs as four textural types: (1) replacement of large plagioclase phenocrysts intergrown with minor sericite (M96-11pl), (2) plagioclase microphenocrysts replaced by adularia with no sericite, (3) mixture of fine-grained quartz and adularia replacing the groundmass and (4) in veins and cavities intergrown with quartz as coarse-grained rhombs 30–300 μm long with minor sericite (M96-11). Total fusion ages of M97-02 and M96-11 are indistinguishable: 31.91 ± 0.40 Ma and 31.78 ± 0.23 Ma, respectively (Table 1). Incremental heating of sample M97-02 yielded a nearly concordant age spectrum with four steps containing 76.1% of the ^{39}Ar giving a plateau age of 32.09 ± 0.21 Ma (Fig. 3). These ages overlap that of associated trachytic dykes (32.06 ± 0.13 Ma; Table 1) and are consistent with field observations that magmatic and hydrothermal activity were channelized along the same structures. Experiments on M96-11 and M96-11pl gave discordant age spectra, the former similar to that of the Harman Kaya K-feldspar (Fig. 3), with apparent ages increasing from 27–30 Ma at lower temperature to a maximum age of 33.8 Ma, suggesting that the sample experienced partial ^{40}Ar loss. Seven of ten steps from M96-11 defined a plateau of 32.57 ± 0.14 Ma, but this is older than the $^{40}Ar/^{39}Ar$ age obtained from the host trachytic dykes (32.06 ± 0.13 Ma) and the plateau age (32.09 ± 0.21 Ma) of sample M97-02 (Fig. 3). Because of this discrepancy, we believe that this age is slightly too old. We believe that the plateau age from M97-02 adularia (32.09 ± 0.21 Ma) gives the best estimate of time elapsed since formation of the adularia–sericite mineralization.

Vein alunite–advanced argillic alteration Sample M96-6 comprises coarse-grained alunite with subordinate woodhousite and svanbergite from a small vein located 200 m east of the Harman Kaya monzonite. Replicate incremental heating experiments produced similar strongly discordant age spectra with apparent ages increasing from *c.* 13–15 Ma at low temperature to maximum ages of *c.* 30.4 Ma (Fig. 4). These age spectra suggest a loss of radiogenic argon possibly due to later reheating, or weathering. Thus, even the maximum age of *c.* 30.4 Ma is probably only a minimum for the time since deposition of alunite. A sample of alunite from the same locality was measured by conventional K–Ar methods (McCoyd 1995) and gave an imprecise age of 32.6 ± 1.2 Ma (2σ).

Discussion

Thermal event at 12–13 Ma

The age of the first low-temperature step (13.65 ± 0.5) of the strongly disturbed $^{40}Ar/^{39}Ar$ age spectrum of the Madjarovo alunite coincides with the ages of several other samples from Madjarovo and neighbouring areas: (1) 13.0 ± 0.5 Ma and 13.7 ± 0.6 Ma ages of two sericite separates of sericite alteration and 12.2 ± 1.0 Ma of the sericite from the quartz–sericite vein alteration obtained by McCoyd (1995) using the K–Ar method, (2) 12 Ma Rb–Sr isochron age of a biotite–muscovite gneiss from the lower sedimentary–volcanoclastic part of the Reseda Tuff (Pljusnin *et al.* 1988). Thus, it appears that sericite and alunite experienced partial ^{40}Ar loss at about 12–13 Ma, recording a thermal effect that is distinct in time from the magmatic and hydrothermal activity of Madjarovo volcano. It deserves noting that earlier, Kasukeev *et al.* (1979) recorded an identical thermal event (12 ± 4–16 ± 5 Ma) in the mica-bearing pegmatites from Kamilski Dol, an area about 20 km east of Madjarovo, using the fission track method. Disturbed ages of adularia M96–11 also seen to reflect this thermal event. The only important difference between adularia samples M97-02 and M96-11 is their position with respect to metamorphic basement. Sample M97-02, is located approximately 500–600 m above the metamorphic basement, whereas sample M96-11 is less than 50 m above the metamorphic basement. All the other samples showing disturbed $^{40}Ar/^{39}Ar$ age spectra or younger ages (e.g. McCoyd's sericites and Pliyusnin *et al.*'s biotite–muscovite gneiss from the Reseda Tuff) are taken either close to or directly from the metamorphic basement, suggesting that the ^{40} Ar loss is not consistent with supergene processes.

The closure temperatures for argon diffusion in muscovite and sericite depend mainly on the temperature and to a lesser extend on the cooling rate, being higher for rapid cooling and lower for slow cooling (Dodson 1973). Snee *et al.* (1988) estimated a muscovite argon closure temperature of about 325 °C under conditions of rapid cooling and short reheating and a temperature of about 270 °C during slow cooling or extended reheating. The biotite $^{40}Ar/^{39}Ar$ ages indicate that there was no heating above 300 °C. The low-temperature release can be facilitated by the fine-grained size of the sericite. However, although this may be applicable to the sericite in the quartz–sericite alteration it is not thought to apply to the coarser-grained muscovite in the metamorphic rocks. In a study of fluid disturbed ages in metamorphic rocks Miller *et al.* (1991) state that a convecting fluid at approximately 275 °C may have caused the loss of radiogenic argon from samples of muscovite with the amount lost dependant upon the length of time the mineral remained at this temperature.

Our preferred explanation for the age difference between disturbed and non-disturbed rocks at Madjarovo is a partial resetting of K–Ar isotope system in the muscovite and alunite that occurred 12–13 Ma ago as the result of endogenous processes.

Duration of magmatic and hydrothermal activity

Our $^{40}Ar/^{39}Ar$ data constrain the duration of magmatic activity and the timing of principal magmatic/hydrothermal events in the complex. Volcanism began shortly after emplacement of the Reseda tuff at 32.44 ± 0.23 Ma. The biotite single-crystal ages of 32.66 ± 0.14 Ma and 32.69 ± 0.15 Ma (Table 1) from the lowermost latite lava combined with the plateau age of 32.72 ± 0.12 Ma (Fig. 3) are indistinguishable at the 95% confidence level from the underlying Reseda Tuff, implying that the two events were closely spaced in time. The ages of 32.23 ± 0.19 Ma and 32.16 ± 0.08 Ma (Fig. 3, Table 1) from the uppermost lavas agree with the 32.16 ± 0.15 Ma age of the Borovitsa pyroclastic flow that covers these lavas (Singer & Marchev 2000). The last volcanism was accompanied or followed by the intrusion of the Harman Kaya stock and trachytic dykes *c.*32.2?–32.06 ± 0.13 Ma. Association of the stock with this volcanism is supported by their similar Sr and Nd isotope ratios (Marchev *et al.* 2002).

Thus, magmatic activity took place over a period of not more than 900 ka, most probably *c.*500 ka which falls well within the lifespan of well-documented composite volcanoes in Japan, the Cascades, and Southern Andes that were active for 80 ka to 900 ka (e.g., Wohletz & Heiken 1992; Singer *et al.* 1997).

Hydrothermal activity began with intrusion of the monzonite stock (*c.*32.2? Ma) and trachytic dykes (32.06 ± 0.13 Ma) and created the advanced argillic (>30.4 Ma) and adularia–sericite alteration/mineralization (32.09 ± 0.21), respectively. The loss of Ar in the alunite did not allow dating of the advanced argillic alteration. However, two types of alteration spatially overlap in the central part of the volcano with cross-cutting relationships, suggesting that adularia–sericite postdates the lithocap formation. The emplacement of trachytic dykes at 32.06 ± 0.13 Ma and subsequent adularia alteration at 32.09 ± 0.21 Ma indicate that the duration of both the advanced argillic, and adularia–sericite systems was less than 250 ka.

This includes time for the monzonite stock to cool, solidify, and develop advanced argillic and sericite alteration. Numerical modelling (Cathles *et al.* 1997; Marsh *et al.* 1997) indicates that a shallow stock of this size would cool below the closure temperature of dateable minerals in less than 100 ka.

The Madjarovo epithermal system

Alteration and epithermal deposits traditionally have been divided into acid sulphate or high-sulphidation and adularia–sericite or low-sulphidation (Heald *et al.* 1987; Hedenquist *et al.* 2000 and references therein). Hedenquist *et al.* (2000, 2001), partly based on the studies of John *et al.* (1999) and John (2001), add another type, dividing the low-sulphidation epithermal deposits into intermediate-sulphidation and proper low-sulphidation deposits. According to these authors, the intermediate-sulphidation deposits are typically hosted in arc-related andesites and dacites. Mineralization is Ag and base-metal rich with Mn carbonates and barite as gangue and massive to comb textured quartz. Sericite is a common alteration and gangue mineral but adularia is rare. Salinity of fluid inclusions is from 3–5 to 10–20 wt% NaCl. Typical low-sulphidation deposits formed in extensional settings hosted by rhyolitic–dacitic or more alkaline rocks. They are Au-rich with the sulphides (pyrite, pyrrotite, arsenopyrite, and high-Fe sphalerite) recording a low-sulphidation state. Veins show crustiform textures with dominated chalcedony, whereas adularia and illite are common gangue and alteration minerals. The salinity of the fluids is generally <1 wt% NaCl.

Based on the high Ag content and barite, sulphide mineralization (including the Fe-poor sphalerite), zonation of the deposit, and salinity of the fluids, the epithermal mineralization at Madjarovo should be an intermediate-sulphidation type. However, Madjarovo is distinguished in having extensive adularia–sericite alteration, a small amount of carbonate, extensional structures, and shoshonitic volcanism, which are more typical of low-sulphidation systems.

Comparison with other high-, low-, and intermediate-sulphidation systems

Although Heald *et al.* (1987) argue that the adularia–sericite and acid–sulphate environments are mutually exclusive, a number of ore districts preserve both. These deposits originated in different arc settings: ocean island, e.g. the Plio-Pleistocene Baguio volcano, Northern Luzon, Philippines (Aoki *et al.* 1993) and Tavua Caldera, Fiji (Setterfield *et al.* 1992), continental arcs, e.g. Comstock Lode (Vikre 1989); Eocene Mount Skukum Au deposit, Yukon Territory, Canada (Love *et al.* 1998) and Oligocene Chala deposit, Bulgaria (Singer & Marchev 2000). Most of these (Comstock Lode, Baguio and Chala) fall in the intermediate-sulphidation type of Hedenquist *et al.* (2001). The intermediate-sulphidation Victoria deposit, high-sulphidation Lepanto and Far Southeast porphyry Cu–Au deposits in Luzon, Phillipines are additional examples of a close spatial and temporal association between these different types of hydrothermal systems (Arribas *et al.* 1995; Hedenquist *et al.* 1998, 2001). Precise K–Ar dating of K-silicate to sericite alteration in Lepanto–Far Southeast revealed synchronicity of these processes that occurred over less than 100 ka (Hedenquist *et al.* 1998, 2001).

High-precision K–Ar and $^{40}Ar/^{39}Ar$ dating suggests that age differences between the acid-sulphate and adularia–sericite alteration types range from 300 to 800 ka and possibly up to 1.6 Ma (Setterfield *et al.* 1992; Aoki *et al.* 1993; Love *et al.* 1998; Singer & Marchev 2000). The temporal separation at Madjarovo was less than 250 ka and probably less than 100–200 ka. In this respect Madjarovo resembles the Far Southeast–Lepanto–Victoria system, where the intermediate-sulphidation Victoria deposit formed *c.* 150 ka after the Far Southeast porphyry and the Lepanto high-sulphidation deposit (Hedenquist *et al.* 2001).

Changes in alteration and mineralization styles in several epithermal systems were accompanied by shifts from intermediate to silicic magma compositions (Bonham 1986; Sillitoe 1989; McEwan & Rice 1991; Singer & Marchev 2000).

It appears that changes in alteration style at Madjarovo were not related to different magma compositions. The composition and age of monzonite stocks and trachytic dykes are identical, reflecting shallow emplacement of a single batch of magma and its associated hydrothermal system. However, a short time gap between intrusion of trachytic dykes and emplacement of the low-sulphidation mineralization could be enough for a change in the composition of the source magma towards more acid composition (Fig. 5).

The contributions from cooling magmas to low-sulphidation epithermal systems may be restricted to the heat needed to drive hydrothermal circulation. Low-sulphidation hydrothermal systems typically form distal to intrusions and may apparently persist up to 1.5 Ma after volcanism (Silberman 1985; Heald *et al.* 1987; Conrad *et al.* 1993; Hedenquist & Lowenstern 1994). However, based on precise $^{40}Ar/^{39}Ar$ measurements, Conrad & McKee (1996), Henry *et al.* (1997) and Singer &

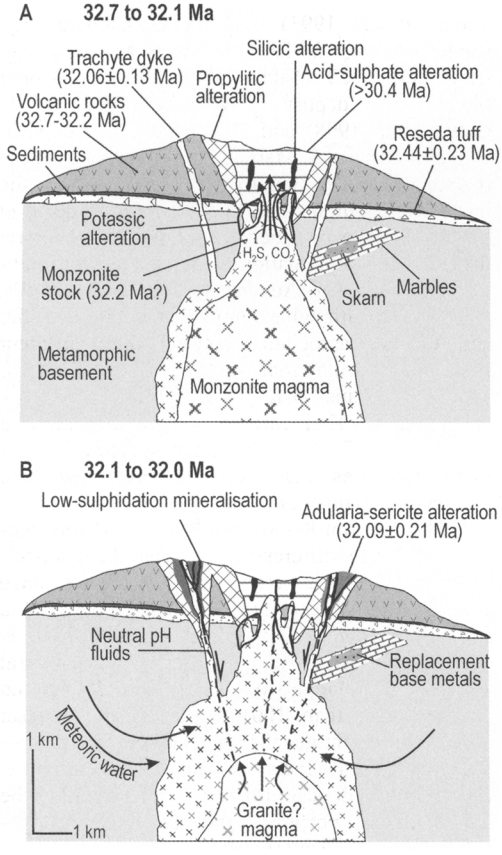

Fig. 5. Model for the evolution of Madjarovo volcanic complex, associated alteration and mineralization.

Marchev (2000) showed that high-grade adularia–sericite deposits at Sleeper and Round Mountain, Nevada and Chala, Bulgaria, were generated 100 ka to 300 ka after emplacement of rhyolitic magmas. Madjarovo deposits are similar, having formed rapidly after trachytic magma intrusion.

A close spatial and temporal relationship between rhyolitic dykes and adularia–sericite alteration/mineralization in the Spahievo Ore District, Bulgaria was interpreted by Singer & Marchev (2000) as reflecting a genetic connection. Similarly, the association of monzonite/trachyte magma and low-sulphidation vein mineralization at Madjarovo is interpreted to favour a direct genetic relationship. However, comparison of the Sr isotope compositions of the monzonite intrusion and gangue barite from the largest veins (Marchev *et al.* 2002) make the Harman Kaya intrusion an unlikely source for the low-sulphidation epithermal system. Thus, we propose that the fluids forming the low-sulphidation mineralization at Madjarovo were related to a magma that solidified at a deeper level, perhaps 3–4 km depth, and that the fluids were additionally contaminated by radiogenic Sr from Rhodope basement rocks which host the intrusions.

Model

Our model for the evolution of the Madjarovo volcanic complex, its alteration and mineralization, is outlined in Figure 5 and summarized here:

1 a shield volcano grew between 32.7 and 32.2 Ma;
2 magmatism continued 32.2–32.1 Ma with intrusion of monzonitic stocks and trachytic dykes, as apophyses of a larger pluton located at depths of 2–4 km (Fig. 5a);
3 intrusion of the latter magma was followed by a period of rapid erosion and down-cutting that removed 300–500 m from the south half of the complex; the palaeosurface encroached the top of the Harman Kay monzonitic stock;
4 the deeper crystallizing volume of the pluton exolved a S- and Cl-rich fluid that separated to form a low-saline acid vapour and saline brine (e.g. Hedenquist & Lowenstern 1994; Shinohara & Hedenquist 1997); acid vapour ascended and reacted with the top of the monzonitic stocks and their host lavas, thereby forming barren lithocap zones; brines also condensed to form K-alteration and minor porphyry mineralization;
5 progressive cooling and fractionation of the pluton produced more silicic (granitic or granosyenitic) magma evinced as the quartz latite lavas; separation, neutralization, and dilution of this mainly magmatic fluid gave rise to the low-sulphidation mineralization; the time span separating intrusion of the monzonite-trachyte magma, formation of lithocap, and the low-sulphidation system was most probably not more than 200 ka.

This work was funded by Swiss NSF Grant 7BUPJ048659 for Bulgarian–Swiss cooperative research. We appreciate the comments and helpful reviews by R. Nakov and M. Economou. The comments and constructive advice of A. von Quadt are greatly acknowledged. We thank Danko Jelev for assistance in the field and Raya Raicheva for help with the figures.

References

Aoki, M., Comsti, E.C., Lazo, F.B. & Matsuhisa, Y. 1993. Advanced argillic alteration and geochemistry of alunite in an evolving hydrothermal system at Baguio, Northern Luzon, Philippines. *Resource Geology*, **43**, 155–164.

ARIKAS, K. & VOUDOURIS, P. 1998. Hydrothermal alterations and mineralizations of magmatic rocks in the southeastern Rhodope massif. *In:* CHRISTOFIDES, G., MARCHEV, P. & SERRI, G. (eds) *Teriary magmatism of the Rhodopian region.* Acta Vulcanologica, **10**, 353–365.

ARNAUDOVA, R., VELINOV, I., GOROVA, M., ARNAUDOV, V., BONEV, I., BATANDJIEV, I. & MARCHEV, P. 1991. Geochemistry of quartz-adularia metasomatites from the Madjarovo Tertiary polymetal Au-Ag deposits, the East Rhodopes. *In:* MRNA, F. (ed.) *Exploration Geochemistry 1990.* Proceedings of the 3rd International Joint Symposium IAGC and AGC, Prague, 13–16.

ARRIBAS, A. JR, HEDENQUIST, J.W., ITAYA, T., OKADA, T., CONCEPCIÓN, R.A. & GARCIA, J.S. JR 1995. Contemporaneous formation of adjacent porphyry and epithermal Cu-Au deposits over 300 ka in northern Luson, Philippines. *Geology*, **23**, 337–340.

ATANASOV, A. 1959. The structure of the lead zinc ore deposit of Madjarovo. *Annuaire de l'Université de Sofia, Géologie*, **52**(2), 313–348. [in Bulgarian with English Summary].

ATANASOV, A. 1962. Mineralization stages, primary zoning and genesis of the complex ore-deposit of Madjarovo. *Annuaire de l'Univversité de Sofia, Géologie*, **55**(2), 229–267. [in Bulgarian with English Summary].

BERGER, B.R. & EIMON, P. 1983. Conceptual models of epithermal precious metal deposits. *In:* SHANKS, W.C. III (ed.) *Volume on unconventional mineral deposits.* Society of Mining Engineers, American Institute of Mining Engineering, 191–205.

BONHAM, H.F. JR 1986. Models for volcanic-hosted epithermal precious metal deposits; a review. *In: Proceedings Symposium 5: Volcanism, Hydrothermal systems and Related Mineralization.* International Volcanological Congress, Auckland, 13–17.

BRESKOVSKA, V., ILIEV, Z., MAVROUDCHIEV, B., VAPTZAROV, I., VELINOV, I. & NOZHAROV, P. 1976. The Madjarovo ore field. *Geochemistry, Mineralogy and Petrology*, **5**, 23–57. [in Bulgarian with English abstract].

BRESKOVSKA, V. & TARKIAN, M. 1993. Mineralogy and fluid inclusion study of polymetallic veins in the Madjarovo ore field, Eastern Rhodope, Bulgaria. *Mineralogy and Petrology*, **49**, 103–118.

BUCHANAN, L.J. 1981. Precious metal deposits associated with volcanic environments in the southwest. *In:* DICKSON, W.R. & PAYNE, W.D. (eds) *Relations of Tectonics to Ore Deposits in the Southwest Cordillera.* Arizona Geological Society Digest, **14**, 237–262.

CATHLES, L.M., ERENDI, H.J. & BARRIE, T. 1997. How long can a hydrothermal system be sustained by a single intrusive event? *Economic Geology*, **92**, 766–771.

CHRISTOFIDES, G., SOLDATOS, T., ELEFTERIADIS, G. & KORONEOS, A. 1998. Chemical and isotopic evidence for source contamination and crustal assimilation in the Hellenic Rhodope plutonic rocks. *In:* CHRISTOFIDES, G., MARCHEV, P. & SERRI, G. (eds) *Tertiary magmatism of the Rhodopian region.* Acta Vulcanologica, **10**, 305–318.

CONRAD, J.E., MCKEE, E.H., RYTUBA, J.T., NASH, J.T. & UTTERBACK, W.C. 1993. Geochronology of the Sleeper deposit, Humboldt County, Nevada: Epithermal gold-silver mineralization following emplacement of a silicic flow-dome complex. *Economic Geology*, **88**, 317–327.

CONRAD, J.E. & MCKEE, E.H. 1996. High-precision $^{40}Ar/^{39}Ar$ ages of rhyolitic host rocks and mineralized veins at the Sleeper Deposit, Humbolt County, Nevada. *In:* COYNER, A.R. & FAHEY, P.L. (eds) *Geology and ore Deposits of the American Cordilera.* Geological Society of Nevada Symposium Proceedings, Reno/Sparks, Nevada, April 1995, 257–262.

COOKE, D.R. & SIMMONS, S.F. 2000. Characteristics and Genesis of Epithermal Gold Deposits. *Society of Economic Geologists, Reviews in Economic Geology*, **13**, 221–244.

DEL MORO, A., KYRIAKOPOULOS, K., PEZZINO, A., ATZORI, P. & LO GUIDICE, A. 1990. The metamorphic complex associated to the Kavala plutonites: An Rb–Sr geochronological, petrological and structural study. 2nd Hellenic–Bulgarian Symposiun, Thessaloniki. *Geologica Rhodopica*, **2**, 143–156.

DODSON, M.H. 1973. Closure temperature in cooling geochronological and petrological systems. *Contributions to Mineralogy and Petrology*, **40**, 259–274.

DUFFIELD, W. & DALRYMPLE, G.B. 1990. The Taylor Creek Rhyolite of New Mexico: a rapidly emplaced field of lava domes and flows. *Bulletin of Volcanology*, **52**, 475–487.

GERGELCHEV, V.N. 1974. Main features and formation stages of the Madjarovo cauldron subsidence and structural conditions for its ore-bearing properties. *Bulletin of the Geological Institute Series of Metal and Non-metal Mineral Deposits*, **23**, 5–29.

HARKOVSKA, A., YANEV, Y. & MARCHEV, P. 1989. General features of the Paleogene orogenic magmatism in Bulgaria. *Geologica Balcanica*, **19**(1), 37–72.

HEALD, P., FOLEY, N.K. & HAYBA, D.O. 1987. Comparative anatomy of volcanic-hosted epithermal deposits: acid-sulphate and adularia-sericite types. *Economic Geology*, **82**, 1–26.

HEDENQUIST, J.W. & ARRIBAS, A. JR 1999. I. Hydrothermal processes in intrusion-related systems. II. Characteristics, examples and origin of epithermal gold deposits. *In:* MOLNAR, F., LEXA, J. HEDENQUIST, J.W.) (eds) *Epithermal Mineralization of the Western Carpathians.* Society of Economic Geologists, Guidebook Series, **31**, 13–61.

HEDENQUIST, J.W., ARRIBAS, A. JR & REYNOLDS, T.J. 1998. Evolution of an intrusion-centered hydrothermal system, Far Southeast-Lepanto porphyry and epithermal Cu-Mo deposit, Philippines. *Economic Geology*, **93**, 373–404.

HEDENQUIST, J.W., ARRIBAS, A. JR & URIEN-GONZALES, E. 2000. Exploration for epithermal gold deposits. *Society of Economic Geologists, Reviews in Economic Geology*, **13**, 245–277.

HEDENQUIST, J.W., CLAVERIA, R.J. & VILLAFUERTE, G.P. 2001. Types of sulfide-rich epithermal deposits and their affiliation to porfiric systems: Lepanto-

Victoria-Far Southeast deposits, Philippines, as examples. *In: Pro Explo 2001, Lima, Volume Proceedings, CD.*

HEDENQUIST, J.W. & LOWENSTERN, J.B. 1994. The role of magmas in the formation of hydrothermal ore deposits. *Nature*, **370**, 519–527.

HENRY, C.D., ELSON, H.B., MCINTOSH, W.C., HEIZLER, M.T. & CASTOR, S.B. 1997. Brief duration of hydrothermal activity at Round Mountain, Nevada, determined from $^{40}Ar/^{39}Ar$ geochronology. *Economic Geology*, **92**, 807–826.

INNOCENTI, F., KOLIOS, N., MANETTI, P., MAZZUOLI, R., PECCERILLO, A., RITA, F. & VILLARI, L. 1984. Evolution and geodynamic significance of the Tertiary orogenic volcanism in Northeastern Greece. *Bulletin Volcanologique*, **47**, 25–37.

IOSIFOV, D., TSVETKOVA, D., PCHELAROV, V., REVYAKIN, P., GERGELCHEV, V. & TSVETKOV, A. 1987. Deep structure of Avren-Madzarovo ore zone. *Review of the Bulgarian Geological Society*, **48**(2), 73–86. [in Bulgarian with English abstract].

IVANOV, R. 1960. [Magmatism in the East Rhodopean depression: I. Geology]. *Travaux sur la Géolologie de Bulgarie, Série Géochemie et des cÎtes métallliféres et non-métalliféres*, **1**, 311–387. [in Bulgarian with German abstract].

IVANOV, R. 1968. Zonal Arrangement of Rock Series with respect to Deep-Seated Masses. *Repr 23rd International Geological Congress, Prague*, **1**, 43–56.

IVANOV, R. & KOPP, K.-O. 1969. Das Alttertiar Thrakiens und der Ostrhodope. *Geologica et Palaeontologica*, **3**, 123–151.

JOHN, D.A. 2001. Miocene and Early Pliocene epithermal gold-silver deposits in the Northern Great Basin: Characteristics, distribution, and relationship to magmatism. *Economic Geology*, **96**, 1827–1854.

JOHN, D.A., GARSIDE, L.J. & WALLACE, A.R. 1999. Magmatic and tectonic setting of late Cenozoic epithermal gold-silver deposits in Northern Nevada, with an emphasis on the Rah Rah and Virginia ranges and the Northern rift. *Geological Society of Nevada, Special Publications*, **29**, 65–158.

KASUKEEV, N., AMOV, B., KASUKEEVA, M., TANEVA, T. & IGNATOVA, R. 1979. Thack-method studies on the geological age of mica-bearing pegmatites from the Eastern Rhodope Mountains. *Geochimistry, Mineralogy and Petrology*, **10**, 3–10.

LILOV, P., YANEV, Y. & MARCHEV, P. 1987. K/Ar dating of the Eastern Rhodope Paleogene volcanism. *Geologica Balcanica*, **17**(6), 49–58.

LOVE, D.A., CLARK, A.N., HODGSON, C.J., MORTENSEN, J.K., ARCHIBALD, D.A. & FARRAR, E. 1998. The timing of adularia-sericite-type mineralization and alunite-kaolinite-type alteration, Mount Skukun epithermal gold deposit, Yukon Territory, Canada. $^{40}Ar/^{39}Ar$ and U-Pb geochronology. *Economic Geology*, **93**, 437–462.

MARCHEV, P., DOWNES, H., THIRLWALL, M.F. & MORITZ, R. 2002. Small-scale variations of $^{87}Sr/^{86}Sr$ isotope composition of barite in the Mafjarovo low-sulphidation epithermal system, SE Bulgaria: implications for sources of Sr, fluid fluxes and pathways of the ore-forming fluids. *Mineralium Deposita*, **37**, 669–677.

MARCHEV, P., ILIEV, Z. & NOKOV, S. 1989. Oligocene volcano Madjarovo. *Guide-book of Scientific excursion*, **E-2**, 97–103.

MARCHEV, P., NOKOV, S., MCCOYD, R. & JELEV, D. 1997. Alteration processes and mineralizations in the Madjarovo Ore Field - a brief review and new data. *Geochimistry, Mineralogy and Petrology*, **32**, 47–58.

MARCHEV, P. & ROGERS, G. 1998. New Rb-Sr data on the bottom and top lava flow of the Madjarovo volcano: Inferences for the age and genesis of the lavas. *Geochimistry, Mineralogy and Petrology*, **34**, 91–96.

MARCHEV, P., ROGERS, G., CONREY, R., QUICK, J., VASELLI, O. & RAICHEVA, R. 1998a. Paleogene orogenic and alkaline basic magmas in the Rhodope zone: relationships, nature of magma sources, and role of crustal contamination. *In:* CHRISTOFIDES, G., MARCHEV, P. & SERRI, G. (eds) *Tertiary magmatism of the Rhodopian region*. Acta Vulcanologica, **10**, 217–232.

MARCHEV, P., VASELLI, O., DOWNES, H., PINARELLI, L., INGRAM, G., ROGERS, G. & RAICHEVA, R. 1998b. Petrology and geochemistry of alkaline basalts and lamprophyres: implications for the chemical composition of the upper mantle beneath the Eastern Rhodopes (Bulgaria). *In:* CHRISTOFIDES, G., MARCHEV, P. & SERRI, G. Acta Vulcanologica, **10**, 233–242.Tertiary magmatism of the Rhodopian region.

MARSH, T.M., EINAUDI, M.T. & MCWILLIAMS, M. 1997. $^{40}Ar/^{39}Ar$ geochronology of Cu-Au and Au-Ag mineralization in the Potrerilos district, Chile. *Economic Geology*, **92**, 784–806.

MAVROUDCHIEV, B. 1959. Upper Oligocene intrusions from the Madjarovo ore district. *Annuaire de l'Université de Sofia, Géologie*, **52**(2), 251–300. [in Bulgarian with English Summary].

MAVROUDCHIEV, B., BOYANOV, I., JOSSIFOV, D., BRESCOVSKA, V., DIMITROV, R. & GERGELCHEV, V. 1996. Late Alpine Metallogeny of the Eastern Rhodope Collision-collapse units and Continental-rift Structures. *In:* POPOV, P. (ed.) *Plate tectonic aspects of the Alpine metallogeny in the Carpatho-Balkan region*. Sofia, UNESCO, IGCP Project N356, **1**, 125–135.

MCCOYD, R. 1995. *Isotopic and geochemical studies of the epithermal-mesothermal Pb-Zn deposits of S.E. Bulgaria*. PhD thesis, University of Aberdeen.

MCEWAN, C.J.A. & RICE, C.M. 1991. Trace-element geochemistry and alteration facies associated with epithermal gold-silver mineralization in an evolving volcanic centre, Rosita Hills, Colorado, U.S.A. *Transactions of the Institution of Mining and Metallurgy*, **100**, B19–B27.

MILLER, W., FALLICK, A., LEAKE, B., MACINTYRE, R. & JENKIN, G. 1991. Fluid disturbed hornblende K-Ar ages from Dalradian rock of Connemara, Western Ireland. *Journal of the Geological Society, London*, **148**, 985–992.

NOKOV, S. & MALINOV, O. 1993. Quartz-adularia metasomatites and molybdenium mineralization from the Madjarovo ore field (SE Bulgaria). *Review*

of the Bulgarian Geological Society, **54**(1), 1–12.

PLJUSNIN, G.S., MARCHEV, P. & ANTIPIN, V.S. 1988. Rb-Sr age and genesis of the shoshonite-latite Eastern Rhodopes series. *Doklady Akademii Nauk SSSR*, **303**, 719–724.

RADONOVA, T. 1960. [Studies on the mineral composition and alterations of Madjarovo base-metal ore deposit in the Eastern Rhodopes]. *Travaux sur la Géolologie de Bulgarie, Série Géochemie et des cÎtes métallifères et non-métallifères*, **1**, 115–197. [in Bulgarian with German abstract].

RAICHEVA, R., MARCHEV, P. & VASELLI, O. 2001. Mixed and mingled lavas at Lower Oligocene Madjarovo and Zvezdel volcanoes, Eastern Rhodopes (Bulgaria). ABCD-GEODE 2001 Workshop Vata Bai, Romania. *Romanian Journal of Mineral Deposits*, **79**(suppl. 2), 88–89.

RICOU, L-E. 1994. Tethys reconstructed: plates, continental fragments and their boundaries since 260 Ma from Central America to Southeastern Asia. *Geodinamica Acta*, **7**, 169–218.

SETTERFIELD, T.H., MUSSETT, A. & OGLETHORPE, R.D.J. 1992. Magmatism and associated hydrothermal activity during the evolution of the Tavua Caldera: $^{40}Ar/^{39}Ar$ dating of the volcanic, intrusive, and hydrothermal events. *Economic Geology*, **87**, 1130–1140.

SHINOHARA, H. & HEDENQUIST, J.W. 1997. Constraints on magma degassing beneath the Far Southeast porphyry Cu-Au deposit, Philippines. *Journal of Petrology*, **38**, 1741–1752.

SILBERMAN, M.L. 1985. Geochronology of hydrothermal alteration and mineralization: Tertiary epithermal precious-metal deposits in the Great Basin. *U.S. Geological Survey Bulletin*, **1646**, 55–70.

SILLITOE, R.H. 1989. Gold deposits in western Pacific island arcs: The magmatic connection. *In:* KEAYS, R.R., RAMSAY, W.R.H. & GROVES, D.I. (eds) *The Geology of Gold Deposits. The perspective in 1988*. Economic Geology Monographs, **6**, 274–291.

SILLITOE, R.H. 1993. Intrusion-related gold deposits. *In:* FOSTER, R.P. (eds) *Gold metallogeny and exploration*. Chapman and Hall, London, 168–208.

SILLITOE, R.H. 1995. Exploration of porphyry copper lithocaps. *In:* MAUK, J.L. & ST GEORGE, J.D. (eds) *PACRIM Congress 1995*. Australasian Institute of Mining and Metallurgy, Publication Series, **9/95**, 527–532.

SINGER, B.S., DUNGAN, M.A. *ET AL.* 1997. Volcanism and erosion during the past 930 thousand years at the Tatara–San Pedro complex, Chilean Andes. *Geological Society of America Bulletin*, **109**, 127–142.

SINGER, B. & MARCHEV, P. 2000. Temporal evolution of arc magmatism and hydrothermal activity, including epithermal gold veins, Borovitsa caldera, southern Bulgaria. *Economic Geology*, **95**, 1155–1164.

SNEE, L.W., SUTTER, J.F. & KELLY, W.C. 1988. Thermochronology of economic mineral deposits: Dating the stages of mineralization at Panasqueira, by high-precision $^{40}Ar/^{39}Ar$ age spectrum techniques on muscovite. *Economic Geology*, **83**, 335–354.

STOYANOV, R. 1979. *[Metallogeny of the Rhodope Central Massif]*. Nedra, Moscow [in Russian].

VELINOV, I. & ASLANIAN, S. 1981. Vein-type alunite from Bulgaria. *Comptes rendus de l'Académie bulgare des Sciences*, **34**, 1417–1419.

VELINOV, I., BATANDJIEV, I., TCHOLAKOV, P. & BLAZHEV, B. 1977. [New data about the relationships between structure forming and postmagmatic processes in Madjarovo ore field]. *Comptes rendus de l'Académie bulgare des Sciences*, **30**, 1749–1752. [in Russian].

VELINOV, I. & NOKOV, S. 1991. Main types and metallogenic significance of the Madjarovo hydrothermally altered Oligocene volcanics. *Comptes rendus de l'Académie bulgare des Sciences*, **44**(9), 65–68.

VIKRE, P.G. 1989. Fluid-mineral relations in the Comstok Lode. *Economic Geology*, **84**, 1574–1613.

WOHLETZ, K. & HEIKEN, G. 1992. *Volcanology and geothermal energy*. University of California Press, Berkeley.

YANEV, Y., INNOCENTI, F., MANETTI, P. & SERRI, G. 1998. Upper Eocene-Oligocene collision-related volcanism in Eastern Rhodopes (Bulgaria)-Western Thrace (Greece): Petrogenetic affinity and geodynamic significance. *In:* CHRISTOFIDES, G., MARCHEV, P. & SERRI, G. (eds) *Tertiary magmatism of the Rhodopian region*. Acta Vulcanologica, **10**, 279–292.